SCIENCE CHINA
Technological Sciences

•Article•

September 2019 Vol.62 No.9: 1585–1595
https://doi.org/10.1007/s11431-019-9533-y

Robust superhydrophobic polyurethane sponge functionalized with perfluorinated graphene oxide for efficient immiscible oil/water mixture, stable emulsion separation and crude oil dehydration

CAO Ning[1,2*], GUO JingYu[2], BOUKHERROUB Rabah[3], SHAO QingGuo[2], ZANG XiaoBei[2], LI Jin[2], LIN XueQiang[2], JU Hong[2], LIU EnYang[2], ZHOU ChaoFan[2] & LI HuiPing[4]

[1] *Key Laboratory of Unconventional Oil & Gas Development, Ministry of Education, China University of Petroleum (East China), Qingdao 266580, China;*
[2] *School of Materials Science and Engineering, China University of Petroleum (East China), Qingdao 266580, China;*
[3] *Univ. Lille, CNRS, Centrale Lille, ISEN, Univ. Valenciennes, UMR 8520, IEMN, Lille, France;*
[4] *School of Materials Science and Engineering, Shandong University of Science and Technology, Qingdao 266590, China*

Received March 8, 2019; accepted May 29, 2019; published online July 18, 2019

In recent years, graphene oxide (GO), prepared by the modified Hummers' method, and its derivatives have become a focus of research owing to their outstanding physical and chemical properties and low cost. Drawing inspiration from the mussel protein, a facile and environmentally-friendly method was employed to fabricate superhydrophobic/superoleophilic reduced graphene oxide (rGO) derivative. The preparation comprises two steps: coating GO nanosheets with polydopamine (PDA) and subsequent reaction with 1*H*,1*H*,2*H*,2*H*-perfluorodecanethiol. Due to the excellent adhesive ability of PDA, the resulting *f*PDA modified rGO nanosheets (rGO-*f*PDA) were firmly immobilized onto polyurethane (PU) sponge skeleton by a simple drop-coating method. The as-prepared rGO-*f*PDA functionalized sponge exhibited superhydrophobic behavior with a water contact angle of 162°±2°, high organic adsorption capacity, recyclability and stable oil/water separation behavior under different acidic/alkaline conditions. Due to its facile fabrication technique and outstanding properties, the superhydrophobic-superoleophilic PU-rGO-*f*PDA sponge holds great promise as an oil adsorbent for cleaning up large-scale pollution of oil and organic solvents, and dehydrating crude oil.

graphene oxide, superhydrophobic sponge, adsorption, oil/water separation, emulsion

Citation: Cao N, Guo J Y, Boukherroub R, et al. Robust superhydrophobic polyurethane sponge functionalized with perfluorinated graphene oxide for efficient immiscible oil/water mixture, stable emulsion separation and crude oil dehydration. Sci China Tech Sci, 2019, 62: 1585–1595, https://doi.org/10.1007/s11431-019-9533-y

1 Introduction

With the fast development of marine engineering, modern transportation and petrochemical industry, oil spilling and chemical leakage from industrial accidents have generated great impact on marine and aquatic ecosystems. Meanwhile, the effluents from chemical industry have led to excessive levels of organic matter in drinking water, which causes damage to human health. Hence, much attention has been paid to the removal of organic pollutants from water bodies [1–3]. Traditionally, organic pollutants are cleaned up by various adsorbent materials, such as vinyl-coated fabrics, zeolites, polypropylene (PP) sponge and many other adsorbents with microporous structures. However, these materials have many limitations like environmental incompatibility, low adsorption capacity as well as poor recycl-

*Corresponding author (email: caoning@upc.edu.cn)

ability, which hinder their practical uses [4].

With the advantages of high porosity, low density, high adsorption capacity and economic efficiency [5], commercial polyurethane (PU) sponges are often deemed as ideal substrates for the preparation of oil adsorbents. However, they are naturally hydrophilic and are therefore impossible to remove oil selectively from water. Thus, it is necessary to change them from being hydrophilic to hydrophobic so as to achieve efficient separation of oil from water [6,7].

In recent years, more and more attention has been paid to materials with superhydrophobic/superoleophilic properties in the field of oil/water separation [8]. Carbon nanotubes (CNTs) [9], mesh films [10], filter papers [11], graphene and its derivatives [12] have been investigated for oil/water separation. Among these materials, reduced graphene oxide (rGO) displays many excellent properties such as good chemical stability, large surface area, as well as ion exchange properties. Consequently, rGO is promising for a wide variety of potential applications. However, the strong interlayer van der Waals forces of rGO make it hard to disperse in common solvents, which impose great limitations for its applications and processing. rGO is the reduction product of graphene oxide (GO), which is in turn obtained from the oxidation of graphite [13]. Compared with rGO, graphene oxide has an extended layered structure where there are many hydrophilic polar groups (such as hydroxy, carbonyl and carboxyl) bulging from its layers. This unique structure makes GO hydrophilic and thus easily dispersible in water. Meanwhile, these functional groups can act as a secondary platform for further reaction, providing more opportunities for the application of GO in oil/water separation field.

In addition, inspired by the adhesive mussel protein, it has been revealed that dopamine, which contains catechol and amine groups, can form robust interactions on the interface of many kinds of surfaces via self-polymerization in a mild-alkali environment. The resulting polydopamine (PDA) can be used as an ideal substrate for surface modifications, because it has a multitude of active sites on the surface [14–16]. In recent years, polydopamine coatings have become a popular alternative for the preparation of superhydrophobic materials. CNTs, which had been modified with octadecylamine through the combination of Michael addition reaction and mussel-inspired chemistry, were used to reinforce a PU sponge, and the reinforced PU sponge was successfully applied for separating oil/water mixtures [17]. Superhydrophobic melamine sponge which has excellent oil-adsorbing quality was prepared through coating with polydopamine (PDA) thin films and subsequent modification with 1*H*,1*H*,2*H*,2*H*-perfluorodecanethiol [18]. In our previous study, PU sponge functionalized with superhydrophobic nanodiamond was obtained via coating hydroxylated nanodiamond particles with PDA and subsequent reaction with 1*H*,1*H*,2*H*,2*H*-perfluorodecanethiol (PFDT). The functionalized PU sponge exhibited excellent oil/water separation [19]. Also, we fabricated a PDA-functionalized-rGO based aerogel which was reinforced by chitosan and modified by PFDT. During the process, the GO was partially reduced to rGO by PDA, while the PDA was oxidized, which provided more active sites for Michael addition or Schiff base reaction with thiol or amino groups [20].

In this paper, an oil adsorbent PU sponge coated with modified GO was prepared by a facile method. Figure 1 illustrates the chemical approach adopted to prepare the superhydrophobic PU sponge. The self-polymerized PDA thin film was firstly coated onto GO nanosheets in a dopamine alkaline solution through self-polymerization to obtain rGO-PDA. Enriched with amino and catechol groups, the PDA film provides an active surface for secondary Michael addition reaction of the thiol group of PFDT to produce perfluorinated superhydrophobic (rGO-*f*PDA). Ultimately, the rGO-*f*PDA was immobilized onto the skeleton of commercial PU sponge [21,22]. The as-prepared sponge exhibited superhydrophobic property, high organic adsorption capacity, high recyclability and good chemical resistance, which renders this sponge promising in the treatment of oil pollution, oily wastewater and crude oil dehydration.

2 Experimental

2.1 Material

Graphite was supplied by Tianhe Graphite Company (Tianjin, China). Tris(hydroxymethyl)aminomethane (Tris), 1*H*,1*H*,2*H*,2*H*-perfluorodecanethiol (PFDT), dopamine hydrochloride (DA), ethanol, hexadecane, toluene, hexane, chloroform, Brilliant blue and Sudan III were obtained from Sigma-Aldrich (USA) and used without further purification. The diesel was bought from China Petrochemical Corporation (China). The crude oil was obtained from Shengli Oilfield, Shandong Province (China). The PU sponge was obtained from a local market and used as obtained. Ultrapure water (18 MΩ) used in all experiments was prepared by ultra-pure water machine (YL-100BU, Yili water treatment equipment Co., Ltd., China). The ultrasonic cleaner (KQ-400KDE) used in the experiment was provided by Kunshan Ultrasonic Co., Ltd. (China) with the maximum power of 400 W and frequency of 40 kHz.

2.2 Preparation of rGO-fPDA superhydrophobic material

Graphite powder was used to prepare graphene oxide (GO) by a modified Hummers' method [23]. The rGO-*f*PDA was fabricated according to the following procedures. Firstly, a proper amount of GO aqueous solution (1 mg/mL) was dispersed in water by ultrasonication for 2 h to dilute and

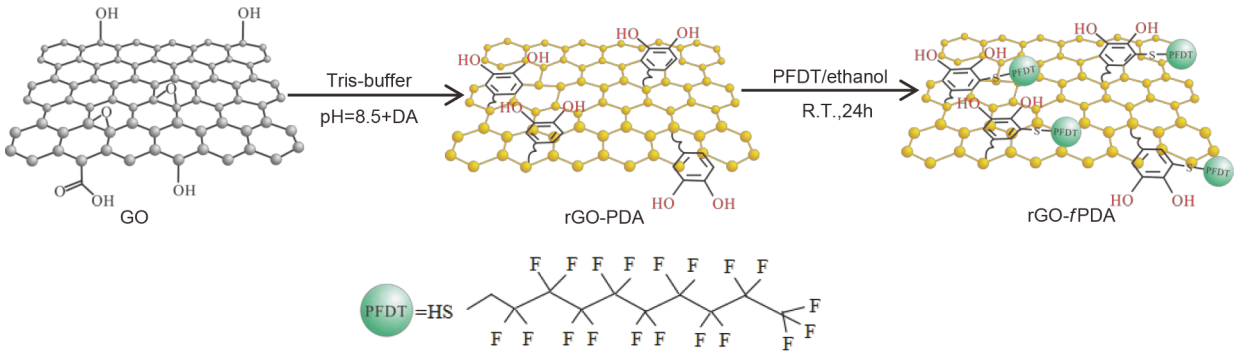

Figure 1 (Color online) Schematic illustration of different steps involved in the preparation of rGO-*f*PDA.

exfoliate the GO sheets thoroughly. Then, Tris powder was added into the GO suspension followed by HCl (10 mmol/L) to adjust its pH value to 8.5. After that, 80 mg of DA was added into 80 mL of the resulting GO/Tris suspension and sonicated at room temperature for 2 h in the ultrasonic bath. Next, the resulting product was separated and collected by means of centrifugation for 40 min at 12000 r/min, and then washed by water and ethanol for two times. The obtained PDA-coated GO (rGO-PDA) was subsequently modified with PFDT (10 mmol/L) in ethanol for 24 h at 25°C. Finally, the rGO-*f*PDA was obtained by means of 2×80 mL of ethanol wash cycles, centrifugation, collection and drying at 50°C.

2.3 Preparation of superhydrophobic PU sponge

The PU sponge with a density below 18 kg/m^3 was cut into blocks with a weight of 10 mg and washed with ethanol ultrasonically. Then, the sponge blocks were cleaned with ultra-purified water and dried in hot air at 70°C. The sponges were immersed in a solution of rGO-*f*PDA (2, 4, 5 and 6 mg) in ethanol (5 mL) and sonicated for 2 h in an ultrasonic bath at room temperature. A series of superhydrophobic sponges with different rGO-*f*PDA loadings were prepared based on the different weight ratio of the rGO-*f*PDA powder to the initial PU sponge. They were then put in a vacuum oven and dried for 24 h at 50°C to obtain a variety of PU sponges reinforced with rGO-*f*PDA.

2.4 Water-in-oil emulsions preparation

Three kinds of water-in-oil emulsions were prepared by mixing water and organic solvents (hexane, toluene, and diesel) at a volume ratio of 1:99 with the addition of 0.15 g/L span 80. Finally, the mixture was subjected to magnetic stirring at 2000 r/min for 6 h. All emulsions were highly stable within 6 h (Figure S1, Supporting Information online).

2.5 Characterization

A DIGIDROP (Zeiss Company, Germany) apparatus was used to measure the contact angle (CA) with 2 μL droplets of water at room temperature. The micro-morphologies of the samples were observed using a field emission scanning electron microscope (FESEM, Nanosem 430, FEI, USA). The element distribution was measured by an energy dispersive spectrometer (Inca X-Max, OXFORD, Britain). A Fourier transform infrared spectrometer (Nicolet 6700, USA) was used to confirm the functional groups of rGO-PDA and rGO-*f*PDA materials. The spectra were recorded by averaging 16 scans (1 min interval) in the range of 500–4000 cm^{-1} at a resolution of 4 cm^{-1} to minimize the effects of dynamic scanning. The elemental composition analysis of rGO-PDA and rGO-*f*PDA was carried out using X-ray photoelectron spectroscopy (ESCALAB 250Xi, USA) with Al Kα radiation ($h\nu$=1486.6 eV). The crystal structure of the rGO-PDA and rGO-*f*PDA was analyzed at 25°C by X-ray diffraction (X'pert PRO XRD, Netherlands) in 2θ degree scan range of 8°–80° at a scanning speed of 4°/min using Cu Kα radiation (λ=0.15417 nm) at a current of 40.0 mA and a voltage of 40.0 kV. The Raman spectra were collected by a Raman spectrometer (Renishaw, Britain) with the laser excitation of 532 nm. Thermogravimetric analysis (TGA) was performed with a METTLER instrument in N_2 atmosphere at a heating rate of 10°C/min. The optical images were captured by a digital camera (Sony, Japan). The distribution of droplet sizes in the emulsion was determined by dynamic light scattering particle size analyzers (Malvern Instruments Ltd., UK).

2.6 Recyclable stability and separation efficiency

The adsorption capacity (Q) of the functionalized PU sponge was determined by the mass ratio of organic liquids (gasoline, diesel, pump oil, ethanol, toluene, chloroform, hexadecane, and hexane) to the functionalized PU sponge, which was calculated using the following formula:

$$Q = \frac{M_e - M_0}{M_0} \times 100\%,$$

where M_e and M_0 represent the sponge weights after and

before the adsorption test respectively.

The functionalized PU sponge separation efficiency (S) was calculated by the following formula:

$$S = \frac{W_a}{W_b} \times 100\%,$$

where W_a and W_b represent the weight of water before and after separation of oil/water mixture, respectively.

The recyclability of the functionalized PU sponge was tested for 10 continuous adsorption-release cycles. The recycle stability was calculated through the following equation:

$$R = \left(1 - \frac{M_{max} - M_{min}}{M_1}\right) \times 100\%,$$

where M_1 represents the weight of adsorbed oil in the first cycle, M_{max} and M_{min} correspond respectively to the maximum and minimum weight of adsorbed oil in the 10 cycles.

The corrosion resistance of the functionalized PU sponges was evaluated through immersion in different aqueous solutions of pH 1–13, boiling water and chloroform for 30 min.

3 Results and discussion

3.1 Perfluorinated graphene (rGO-fPDA) nanosheets

In this study, dopamine was used for GO functionalization in alkaline aqueous solution (pH 8.5). The PDA coating on GO nano-sheets, prepared through self-polymerization of DA at pH 8.5, is a versatile platform for subsequent reactions, allowing to tailor the coating functionalities for multiple applications [15]. Under ambient conditions, catechol/quinone groups of PDA spontaneously react with terminal thiol groups of PFDT via Michael addition reaction to produce a superhydrophobic PDA coating (Figure 1) (more details see section 2 of Supporting Information online).

The characterization of the functionalized GO samples was carried out by means of Fourier Transform infrared spectroscopy (FTIR). FTIR spectra of bare GO, rGO-PDA and rGO-*f*PDA are shown in Figure 2. The strong peaks at 3414, 1738, 1627, 1389, and 1050 cm^{-1} in the GO spectrum were respectively associated with O–H stretching of hydroxy and carboxyl groups, C=O stretching of carboxyl and carbonyl groups, C=C stretching of the unoxidized graphite, O–H bending of hydroxy groups and epoxy C–O stretching [24,25]. After self-polymerization of DA occurred on the GO surface in Tris-HCl solution, the peak at 1738 cm^{-1} disappeared, suggesting the removal of the most oxygen groups. Whereas, additional peaks appeared at 1569 and 1173 cm^{-1}, which was consistent with the main vibrational modes of C=N and C–N of PDA, indicating the formation of a PDA layer on the GO surface. In the FTIR spectrum of rGO-*f*PDA, peaks belonging to –C–F and –C–S–C appeared at 1146 and 1207 cm^{-1}, respectively, confirming PDA functionalization with PFDT molecules.

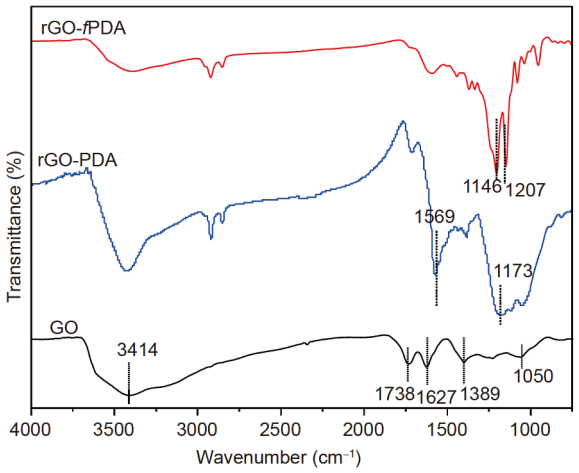

Figure 2 (Color online) Transmission FTIR spectra of GO, rGO-PDA and rGO-*f*PDA.

The XPS survey spectra and quantitative XPS analysis results of rGO-PDA and rGO-*f*PDA are depicted in Figure 3 and Table 1. The spectrum of rGO-PDA (Figure 3(a)) showed strong C 1s, N 1s and O 1s peaks. Successful deposition of PDA on the GO surface was confirmed by the presence of N 1s [26]. Carbon, which is typically present from unavoidable hydrocarbon contamination, was used as an internal reference at 284.6 eV for calibrating peak positions [27]. After PFDT reaction with PDA, two more peaks assigned to F 1s and S 2p appeared in the XPS spectrum along with the O 1s, N 1s and C 1s peaks. The intensity of the XPS peaks of rGO-PDA decreased slightly after the reaction [21]. Figure 3(b) and (c) display the high-resolution C 1s XPS spectrum of rGO-PDA and rGO-*f*PDA. The C 1s spectrum of rGO-PDA was deconvoluted into four different curves with binding energies centered at 284.6 eV (C–C/C–H), 285.1 eV (C–N), 286.6 (C–O) and 288.2 eV (C=O). After PFDT reaction with PDA, peaks assigned respectively to C–H/C–C, C–N, C–O, C=O, CF_2 and CF_3 bonds appeared at 284.3, 285.4, 286.5, 288.1, 291.6 and 293.9 eV. Meanwhile, the peak intensity of C–C/C–H decreased dramatically. Table 1 summarizes the changes of element concentration. After PDA fluorination, the concentrations of nitrogen and carbon decreased significantly from 4.18% and 72.91% to 3.08% and 62.40% for rGO-PDA, while the percentage of sulfur and fluorine increased from 0 to 2.28% and 17.80%, respectively. All the results indicated that *f*PDA had been successfully coated onto GO.

The XRD patterns of GO, rGO-PDA and rGO-*f*PDA are displayed in Figure 4. GO exhibited a sharp diffraction peak at 10.4° with a d-spacing ((001) reflection) of 0.83 nm, which was larger than the interplanar distance of graphite, and this is due to the introduction of oxygen-containing groups during the oxidation process. After reaction with DA, the diffraction peak at 10.4° became broader and weaker,

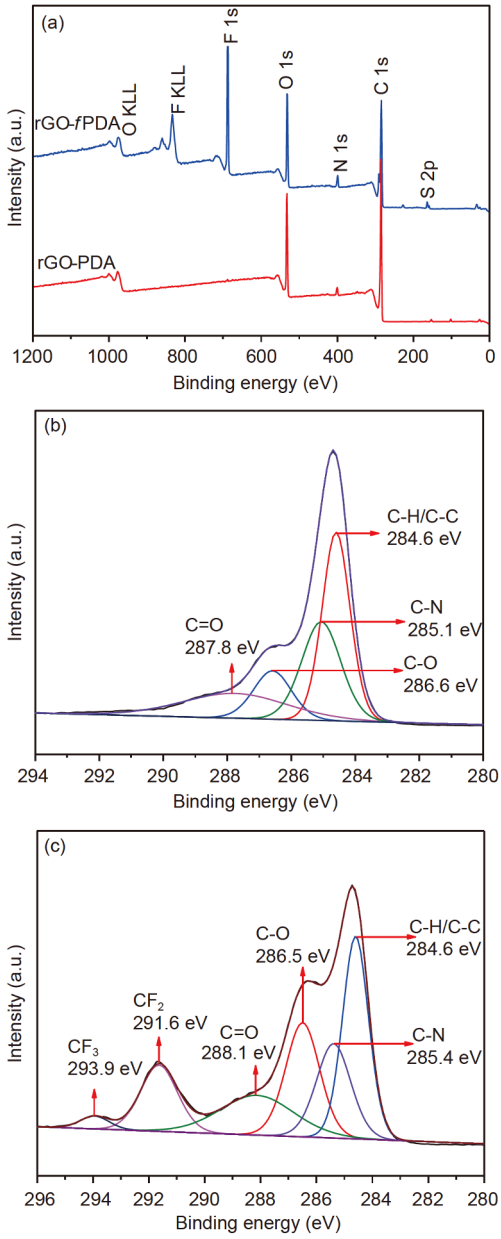

Figure 3 (Color online) XPS spectra of rGO-PDA and rGO-*f*PDA. (a) XPS wide-scan spectra of rGO-PDA and rGO-*f*PDA; typical high-resolution C 1s XPS spectra of (b) rGO-PDA and (c) rGO-*f*PDA.

Table 1 The elemental percentage of rGO-PDA and rGO-*f*PDA

	rGO-PDA (at%)	rGO-*f*PDA (at%)
C 1s	72.91	62.40
O 1s	22.91	14.45
N 1s	4.18	3.08
F 1s	N/A	17.80
S 2p	N/A	2.28

while a broad and weak peak appeared at 2θ=24.6° corresponding to the characteristic peak of rGO, suggesting GO was mostly reduced to rGO [28]. In addition, a new characteristic peak appeared at around 43.1°, which is a fingerprint peak for graphite due to the (100) diffraction [29]. This implies the re-generation of graphitized crystal. The XRD patterns of rGO-PDA and rGO-*f*PDA were similar, indicating that fluorination does not cause further reduction of GO.

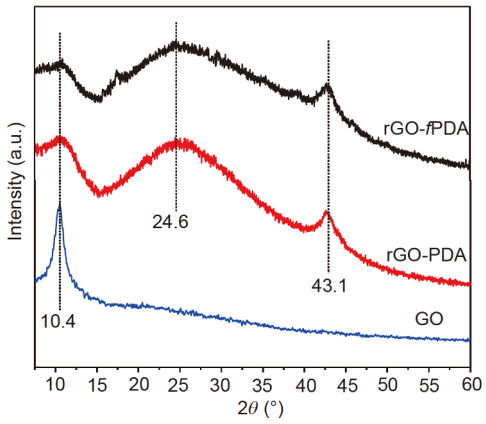

Figure 4 (Color online) XRD patterns of GO, rGO-PDA and rGO-*f*PDA.

Raman spectroscopy was employed to analyze the chemical composition of GO, rGO-PDA, rGO-*f*PDA (Figure 5). All the Raman spectra presented two characteristic peaks at 1347.4 and 1588.9 cm^{-1} due to D-band and G-band of GO. The I_D/I_G ratio was used to evaluate the degree of structural disorder, which was inversely proportional to the size of in-plane crystallite. The calculated I_D/I_G ratio of rGO-PDA (1.01) was larger than that of GO (0.94), indicating that the covalently bonded PDA resulted in increased structural disorder of GO. For the fluorinated rGO-*f*PDA sample, the I_D/I_G increased to 1.09, suggesting that PFDT caused more disordered and defective GO nanostructures.

TGA is a standard technique to determine the thermal stability or composition of materials. Here, TGA of GO, rGO-PDA and rGO-*f*PDA powders was performed to gain a better understanding on how the DA derivatives were linked to the GO surface and/or the bonding strength (Figure 6). The TGA thermogram of GO showed a slow weight loss of 21.6% in the temperature range of 30°C–200°C due to the evaporation of the water adsorbed by the sample. Then, the mass of GO presented a sudden decline of 19.8% at the heating temperature of 200°C due to the disappearance of oxygen-containing functional groups. The mass of the sample decreased slightly within the heating range of 200°C–900°C, and the final residual mass was 32.9% at 900°C. Meanwhile, the rGO-PDA nanostructures were proved to have good thermo-gravimetric stability with a residual mass of 58.15% at 900°C. The TGA analysis of rGO-*f*PDA powder showed a weight loss of 40% between 200°C and 500°C due to the decomposition of organic moieties at temperatures above 220°C. All these results indicated that the rGO-*f*PDA has thermogravimetric stability similar to the primary GO powders.

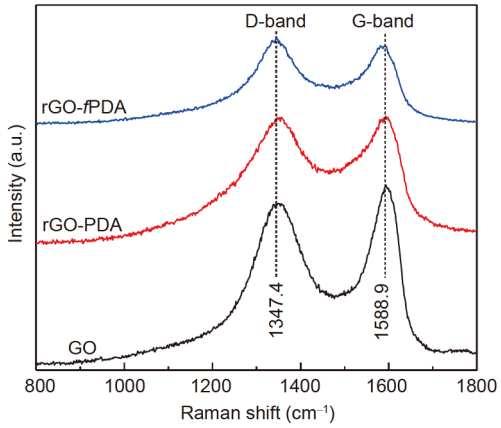

Figure 5 (Color online) Raman spectra of GO, rGO-PDA and rGO-*f*PDA.

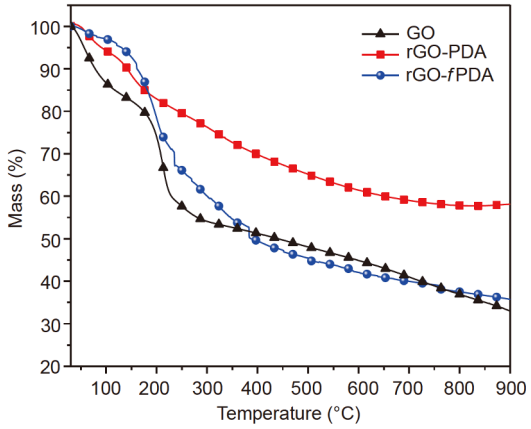

Figure 6 (Color online) TGA curves of GO, rGO-PDA and rGO-*f*PDA.

3.2 Loading of rGO-fPDA powder on PU sponge

In order to study the optimal loading capacity of rGO-*f*PDA powder, different weights of rGO-*f*PDA powder were deposited on PU sponge by repetitive dipping/drying process. The loading capacity, defined as weight ratio W_{powder}/W_{sponge} ×100%, was determined by weighing the original and rGO-*f*PDA coated sponges immediately after drying to prevent moisture adsorption. The relationship between rGO-*f*PDA loading capacity and water contact angle is depicted in Figure 7. The water contact angle of the initial PU sponge was 85°±2°, indicating the hydrophilicity of the PU sponge without modification. The water contact angle reached 125°±2° when the rGO-*f*PDA loading capacity was 20%. When the loading capacity was increased to 40%, the water droplet assumed a spherical shape on the PU surface with the water contact angle (WCA) reaching up to 162°±2°, which suggested its unique feature of superhydrophobicity. With further increase of the loading capacity, the value of contact angle exhibited a sharp decrease.

To understand the wetting behavior of the functionalized

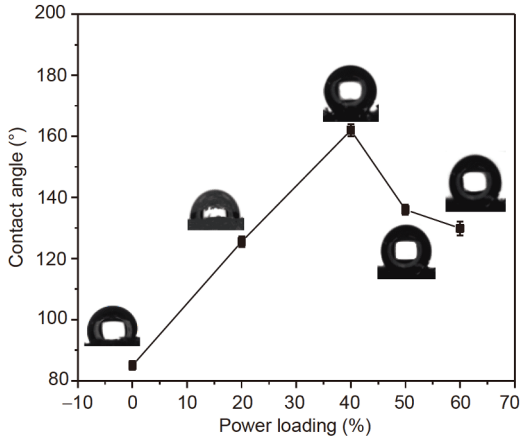

Figure 7 Effect of rGO-*f*PDA loading on the water contact angle of the functionalized PU sponge.

sponge, the PU sponges functionalized with different loadings of rGO-*f*PDA were observed by scanning electron microscopy (SEM). The PU sponge skeletons with the rGO-*f*PDA loading of 20% were very smooth with almost no attached deposit (Figure 8(a_1) and (a_2)). However, with the increase of the rGO-*f*PDA loading, the sponge skeletons became increasingly rough (Figure 8(b_1)–(d_1) and (b_2)–(d_2)). When the loading reached 60%, the loaded rGO-*f*PDA powder began to block the pores of the sponge and destroyed its three-dimensional porous structure, resulting in a decrease in its superhydrophobic property (Figure 8(d_1) and (d_2)). All the results suggested that 40% loading capacity of rGO-*f*PDA was considered to be optimal in obtaining the superhydrophobicity of sponges, and the PU sponge thus obtained was selected for further studies.

The apparent density of non-functionalized PU sponge and that functionalized with rGO-*f*PDA was about (0.029±0.001) g/cm^3 and (0.026±0.001) g/cm^3, respectively. The *dandelion* on which the functionalized PU sponge was placed did not change significantly (Figure S3), suggesting that the density of the functionalized sponge was very small. The compressive strength of the functionalized PU sponge was measured (Figure 9(a)). The compressive elastic strain of the functionalized PU sponge could reach more than 90%, proving that it has excellent flexibility. As shown in Figure 9 (b), after the removal of external force, the functionalized PU sponge restored its original shape (Video S1, Supporting Information online). The functionalized PU sponge has higher compressive strength compared with PU sponge, indicating that the functionalization process improved the mechanical strength.

When completely immersed into water by an external force, the functionalized PU sponge took on a silver mirror-like surface as shown in Figure S4 (refer to Video S3 for more vivid show), which is called the Cassie-Baxter non-wetting behavior because of the generation of an air layer

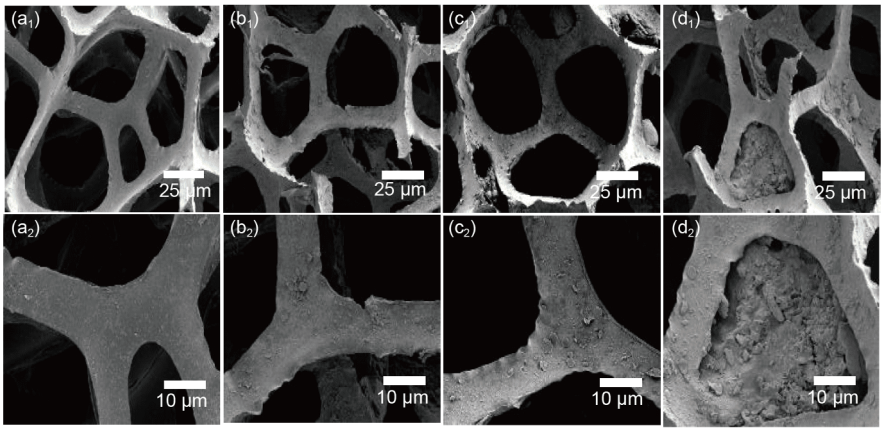

Figure 8 SEM images of PU sponges with (a_1) 20%, (b_1) 40%, (c_1) 50% and (d_1) 60% loading of rGO-*f*PDA, and (a_2)–(d_2) the corresponding SEM images with higher magnification.

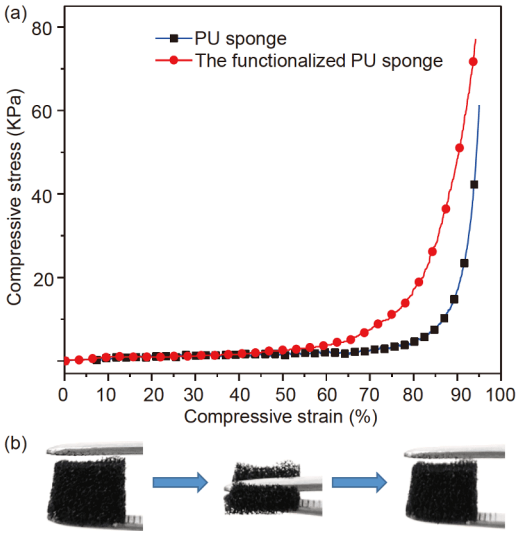

Figure 9 (Color online) Compressive strain-stress curves of PU sponge and the functionalized PU sponge (a), recovery process of the functionalized PU sponge after removal of external force (b).

between the surface of the functionalized PU sponge and water. The moment the external force was removed, the functionalized PU sponge floated on water without any adsorbed water, indicating the superhydrophobic property of the functionalized PU sponge.

The surperhydrophobic character varied depending on different three-dimensional porous structures of the sponge, and microscopic roughness formed as a result of the irregular distribution and stacking of rGO-*f*PDA sheets [30–32]. As shown in Figure 10(a), the structure of the rGO-*f*PDA powder is in lamellar shape with curled wrinkles. It is possible that the reduction of GO by dopamine led to the aggregation of rGO upon the removal of the interlayered epoxy groups. The functionalized sponge exhibited a three-dimensional hierarchical structure composed of irregular pores, and rGO-*f*PDA sheets of wrinkled morphology were distributed homogenously on the PU fibers (Figure 10(b) and (c)), which guaranteed its superhydrophobicity.

The C, N, O and F elements were distributed uniformly on the surface of the functionalized PU sponge, as evidenced by energy dispersive spectroscopy (EDS) mapping (Figure 10 (d)).

3.3 Application of the functionalized sponge for oil adsorption

The efficiency of the functionalized sponge for oil/water separation and adsorption of organic solvents was evaluated. The functionalized PU sponge adsorbed Sudan III dyed toluene within a few seconds (Figure S5(a)–(c), refer to Video S2 for the specific process). And the sponge can also adsorb the high-density organic solvent (chloroform dyed with Brilliant Blue G) from water effectively (Figure S5(d)–(g), Refer to Video S3 for the specific process).

The Q of the functionalized sponges for various organic liquids (including gasoline, diesel, pump oil, ethanol, toluene, chloroform, hexadecane, and hexane) was determined. A weighed amount of sponge was held in contact with an organic liquid until the sponge was completely saturated with the organic liquid. Then the sponge was taken out for weight measurement. The weight measurement was carried out as soon as possible so as to avoid the evaporation of the adsorbed organic liquids, especially those with high vapor pressure.

As shown in Figure 11, the adsorption capacity of the functionalized PU sponge ranges from 21 to 118 for different oils and solvents. The functionalized PU sponges have adsorption capacity comparable to or higher than those reported for different adsorbent systems [19,20,33–36] (Table S1, Supporting Information online), which is attributable to the abundant pores and low-surface-energy material.

Then the capacity of the functionalized PU sponge for oil/water separation was examined (see Video S4). The experiment showed that when the mixture of chloroform dyed by

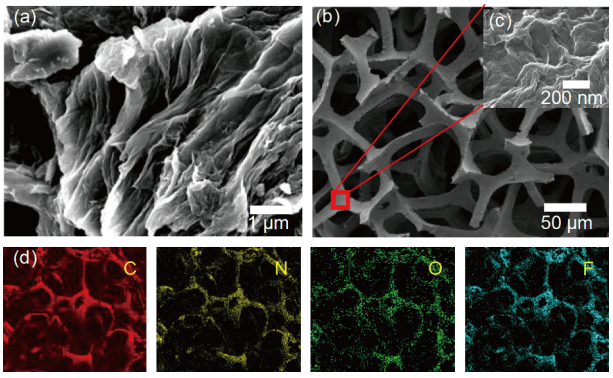

Figure 10 (Color online) SEM images of rGO-*f*PDA powder (a), PU sponge functionalized with rGO-*f*PDA (b) and a zoom on rGO-*f*PDA powder on the PU fibers (c); (d) EDS mapping of PU sponge functionalized with rGO-*f*PDA.

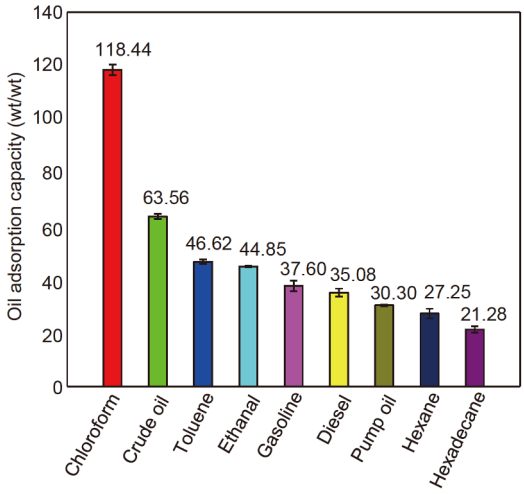

Figure 11 (Color online) Oil adsorption capacity of the functionalized PU sponge.

Sudan red III and water (20% water) was poured onto the functionalized PU sponge filter, the chloroform passed through the filter, and the water stayed on it. This indicated that the functionalized PU sponge had oil/water separation ability and the separation efficiency could reach up to 97% ±1%. Figure 12 depicts a separation of oil and water (50%) mixture.

Additionally, when emulsions were poured onto the functionalized PU sponge filter membrane, the oil passed through the filter under the action of gravity, and the liquid became clear. The microscopic images show that the emulsion comprises a large amount of droplets, which disappear after the filtration, as shown in Figure 13(a)–(c) (see Video S5), and the purity of organic solvents reached around 99.9% as the result of the filtration.

In order to understand the separation effect of the functionalized PU sponge on water-in-oil emulsions, the distribution of droplet size in the filtrate was measured by dynamic light scattering (DLS), as shown in Figure 13(d).

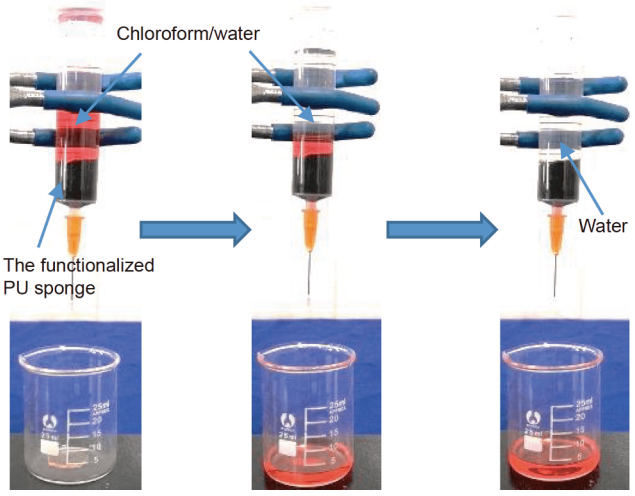

Figure 12 (Color online) Oil/water separation process controlled by the functionalized PU sponge.

The droplet size range of three filtrates was 20–400 nm. The average droplet sizes of water-in-hexane, water-in-toluene, and water-in-diesel filtrates were 132.2, 158.9 and 193.6 nm, respectively, indicating that emulsion can be separated effectively by the functionalized PU sponge.

In addition, we used it to carry out the crude oil dehydration experiment (see Video S6). The 10 mL of crude oil (water content 5%) was poured into a simple device. In less than 4 min, the organic composites of the crude oil passed through the functionalized PU sponge and eventually there was about 0.5 mL of water left on the surface of the sponge in the device. The result showed that the functionalized PU sponge can be employed to successfully separate water from crude oil by gravity.

3.4 Stability of the functionalized PU sponge

Furthermore, the stability of the functionalized PU sponge was determined by measuring the WCA after its immersion into corrosive solutions with pH ranging from 1 to 13 for 30 min. After the sponge was rinsed with pure water and dried, the relationship between WCA and pH value was established. As shown in Figure 14, the water contact angles are larger than 135°, which clearly indicates that the functionalized PU sponge has high stability in corrosive media.

Besides, the functionalized PU sponge had an adsorption capacity of 44 times at pH 1 and 50 times at pH 13 as high as their initial weight after further being used for gasoline adsorption. Meanwhile, the functionalized PU sponge was sealed in a stainless hydrothermal autoclave with the temperature of boiling water kept at 100°C for 30 min, the WCA of the resulting sponge was 156°±2°, while the sponge treated in boiling chloroform had a WCA of 150°±2°, as shown in Figure S6. All the results indicated that the binding force between the rGO-*f*PDA and PU sponge was quite

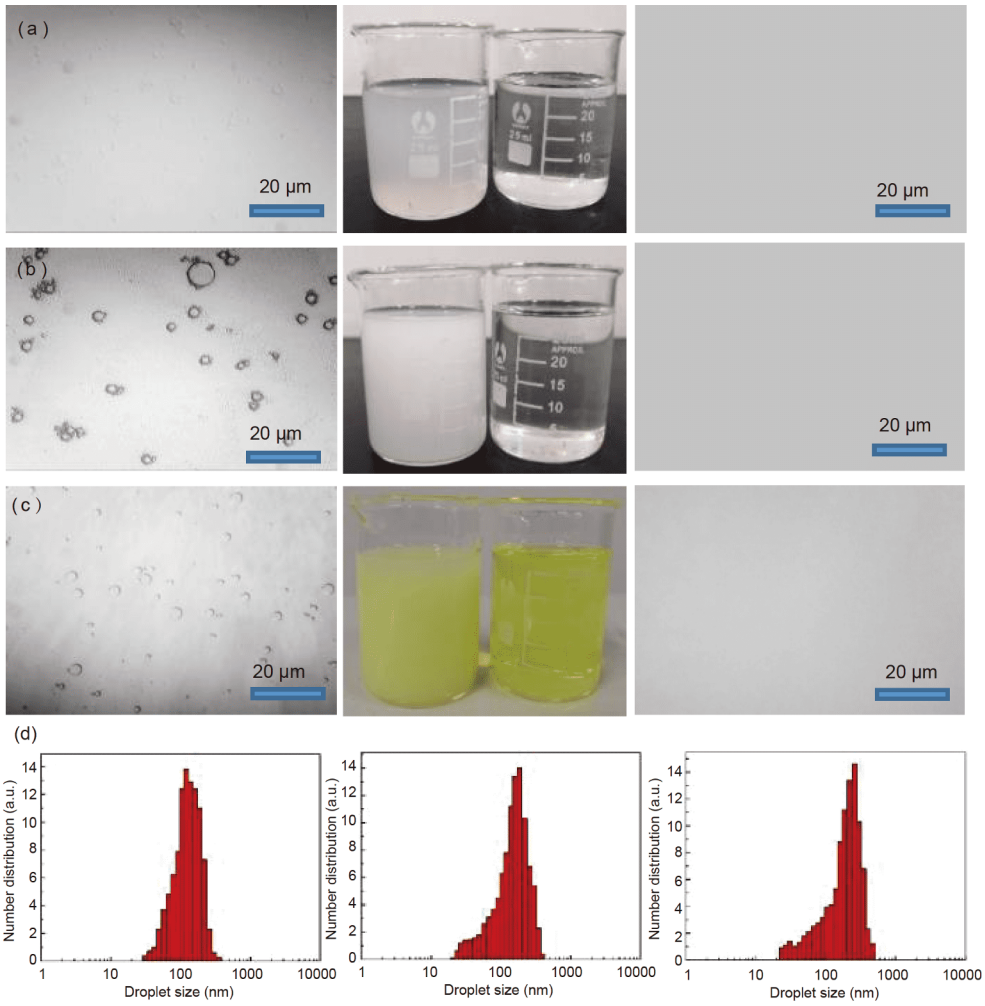

Figure 13 (Color online) (a) Photographs of water-in-hexane emulsion (left) and the collected filtrate (right); (b) photographs of water-in-toluene emulsion (left) and the collected filtrate (right); (c) photographs of water-in-diesel emulsion (left) and the collected filtrate (right); (d) DLS of the collected filtrate: water-in-hexane (left), water-in-toluene (middle), and water-in-diesel (right).

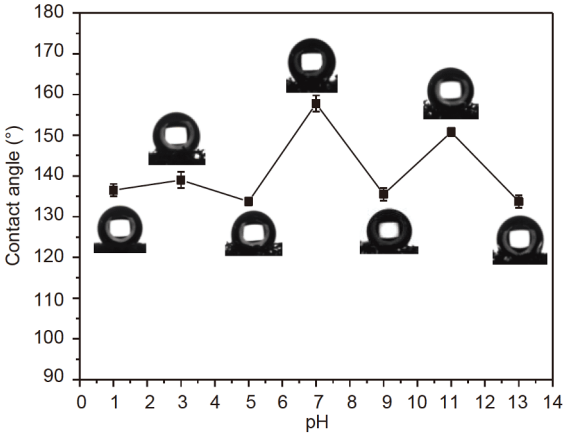

Figure 14 Stability of the functionalized PU sponge at different pH.

strong and the as-prepared sponge was resistant to acidic and alkaline conditions to some degree and was able to adsorb oils from harsh water environment.

3.5 Recyclability of the functionalized PU sponge

The oil-adsorbed sponge is squeezed, dried and reused for the next oil adsorption, so that the adsorbed oil can be collected and the superhydrophobic sponge can be recycled. The recyclability is a highly desirable property in practice. Figure 15 shows the high adsorption capacity and the large WCA of the functionalized PU sponge after 10 consecutive cycles for gasoline, diesel and pump oil with a very small fluctuation and the recyclable stability reached 94.7%, 93.5% and 93.7%, respectively, indicating the high recoverability of the sponge. The porous structure of the functionalized PU sponge before and after 5 oil/water separation cycles is displayed in Figure S7. Obviously, the two PU sponges did not show a great difference in the size and shape of the pores, and the distribution and morphologies of rGO-*f*PDA attached on the sponge skeletons remained almost unchanged, which further confirms the excellent stability and recyclability of the functionalized PU sponge.

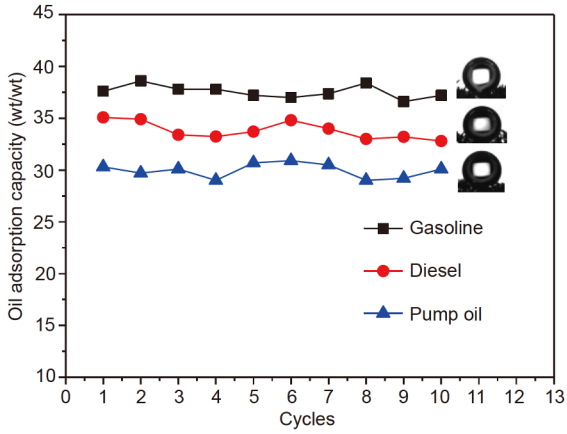

Figure 15 (Color online) The oil adsorption capacity of the functionalized PU sponge after 10 cycles of oil removal process.

4 Conclusion

Inspired by mussel adhesion, a facile and feasible approach was developed to prepare stable superhydrophobic reduced graphene oxide powder through DA self-polymerization and subsequent fluorination using PFDT. The modified GO (rGO-*f*PDA) sheets were firmly immobilized on the skeleton of commercial PU sponge due to excellent adhesive ability of the polydopamine coating. In addition, the as-prepared sponge exhibited superhydrophobic property, high organic adsorption capacity, high recyclability and good chemical resistance. Owing to the economic efficiency, feasible preparation technique and outstanding performance, this kind of superhydrophobic sponge holds great promise as oil adsorbent in cleaning up large-scale pollution of oils and organic solvents from water.

This work was supported by the National Natural Science Foundation of China (Grant Nos. 51701240 & 41206063), Key Research and Development Program of Shandong Province (Grant No. 2017GGX20123), and Fundamental Research Funds for the Central Universities (Grant Nos. 19CX05001A, 16CX05011A & 17CX02063).

Supporting Information

The supporting information is available online at tech.scichina.com and link.springer.com. The supporting materials are published as submitted, without typesetting or editing. The responsibility for scientific accuracy and content remains entirely with the authors.

1 Song S K, Shon Z H, Kim Y K, et al. An oil spill accident and its impact on ozone levels in the surrounding coastal regions. Atmos Environ, 2011, 45: 1312–1322
2 Baig U, Matin A, Gondal M A, et al. Facile fabrication of superhydrophobic, superoleophilic photocatalytic membrane for efficient oil-water separation and removal of hazardous organic pollutants. J Clean Prod, 2019, 208: 904–915
3 Venkataraman P, Tang J, Frenkel E, et al. Attachment of a hydrophobically modified biopolymer at the oil-water interface in the treatment of oil spills. ACS Appl Mater Interfaces, 2013, 5: 3572–3580
4 Zhu Q, Pan Q, Liu F. Facile removal and collection of oils from water surfaces through superhydrophobic and superoleophilic sponges. J Phys Chem C, 2011, 115: 17464–17470
5 Chu Y, Pan Q. Three-dimensionally macroporous Fe/C nanocomposites as highly selective oil-absorption materials. ACS Appl Mater Interfaces, 2012, 4: 2420–2425
6 Yuan S J, Zhang J J, Fan H X, et al. Facile and sustainable shear mixing/carbonization approach for upcycling of carton into superhydrophobic coating for efficient oil-water separation. J Clean Prod, 2018, 196: 644–652
7 Wang J, Zheng Y. Oil/water mixtures and emulsions separation of stearic acid-functionalized sponge fabricated via a facile one-step coating method. Sep Purif Technol, 2017, 181: 183–191
8 Yao X, Song Y, Jiang L. Applications of bio-inspired special wettable surfaces. Adv Mater, 2011, 23: 719–734
9 Gui X, Wei J, Wang K, et al. Carbon nanotube sponges. Adv Mater, 2010, 22: 617–621
10 Feng L, Zhang Z, Mai Z, et al. A super-hydrophobic and super-oleophilic coating mesh film for the separation of oil and water. Angew Chem Int Ed, 2004, 43: 2012–2014
11 Wang S, Li M, Lu Q. Filter paper with selective absorption and separation of liquids that differ in surface tension. ACS Appl Mater Interfaces, 2010, 2: 677–683
12 Bi H, Xie X, Yin K, et al. Spongy graphene as a highly efficient and recyclable sorbent for oils and organic solvents. Adv Funct Mater, 2012, 22: 4421–4425
13 Novoselov K S, Geim A K, Morozov S V, et al. Two-dimensional gas of massless dirac fermions in graphene. Nature, 2005, 438: 197–200
14 Lee H, Dellatore S M, Miller W M, et al. Mussel-inspired surface chemistry for multifunctional coatings. Science, 2007, 318: 426–430
15 Liu Y, Ai K, Lu L. Polydopamine and its derivative materials: Synthesis and promising applications in energy, environmental, and biomedical fields. Chem Rev, 2014, 114: 5057–5115
16 Cao N, Miao Y, Zhang D, et al. Preparation of mussel-inspired perfluorinated polydopamine film on brass substrates: Superhydrophobic and anti-corrosion application. Prog Org Coat, 2018, 125: 109–118
17 Wang H, Wang E, Liu Z, et al. A novel carbon nanotubes reinforced superhydrophobic and superoleophilic polyurethane sponge for selective oil-water separation through a chemical fabrication. J Mater Chem A, 2014, 3: 266–273
18 Fei B, Qian B, Yang Z, et al. Coating carbon nanotubes by spontaneous oxidative polymerization of dopamine. Carbon, 2008, 46: 1795–1797
19 Cao N, Yang B, Barras A, et al. Polyurethane sponge functionalized with superhydrophobic nanodiamond particles for efficient oil/water separation. Chem Eng J, 2017, 307: 319–325
20 Cao N, Lyu Q, Li J, et al. Facile synthesis of fluorinated polydopamine/chitosan/reduced graphene oxide composite aerogel for efficient oil/water separation. Chem Eng J, 2017, 326: 17–28
21 Hong D, Bae K E, Hong S P, et al. Mussel-inspired, perfluorinated polydopamine for self-cleaning coating on various substrates. Chem Commun, 2014, 50: 11649–11652
22 Huang N, Zhang S, Yang L, et al. Multifunctional electrochemical platforms based on the michael addition/schiff base reaction of polydopamine modified reduced graphene oxide: Construction and application. ACS Appl Mater Interfaces, 2015, 7: 17935–17946
23 Hummers Jr W S, Offeman R E. Preparation of graphitic oxide. J Am Chem Soc, 1958, 80: 1339
24 Zhu C, Guo S, Fang Y, et al. Reducing sugar: New functional molecules for the green synthesis of graphene nanosheets. ACS Nano, 2010, 4: 2429–2437
25 Bose S, Kuila T, Uddin M E, et al. *In-situ* synthesis and characterization of electrically conductive polypyrrole/graphene nanocomposites. Polymer, 2010, 51: 5921–5928
26 Liu M, Zhou J, Yang Y, et al. Surface modification of zirconia with polydopamine to enhance fibroblast response and decrease bacterial

activity *in vitro*: A potential technique for soft tissue engineering applications. Colloid Surface B, 2015, 136: 74–83
27 Yuan J, Liu X, Akbulut O, et al. Superwetting nanowire membranes for selective absorption. Nat Nanotech, 2008, 3: 332–336
28 Fan Z, Wang K, Wei T, et al. An environmentally friendly and efficient route for the reduction of graphene oxide by aluminum powder. Carbon, 2010, 48: 1686–1689
29 Zhang B, Wang T, Liu S, et al. Structure and morphology of microporous carbon membrane materials derived from poly(phthalazinone ether sulfone ketone). Microporous Mesoporous Mater, 2006, 96: 79–83
30 Guo L P, Sun W, Yu T, et al. Preparation and characteristics of a recycled cement-based superhydrophobic coating with dirt pickup resistance. Sci China Tech Sci, 2015, 58: 1096–1104
31 Jiang L, Zhao Y, Zhai J. A lotus-leaf-like superhydrophobic surface: A porous microsphere/nanofiber composite film prepared by electrohydrodynamics. Angew Chem Int Ed, 2004, 43: 4338–4341
32 Zhang X, Shi F, Niu J, et al. Superhydrophobic surfaces: From structural control to functional application. J Mater Chem, 2008, 18: 621–633
33 Phanthong P, Reubroycharoen P, Kongparakul S, et al. Fabrication and evaluation of nanocellulose sponge for oil/water separation. Carbohyd Polym, 2018, 190: 184–189
34 Yang J, Xia Y, Xu P, et al. Super-elastic and highly hydrophobic/superoleophilic sodium alginate/cellulose aerogel for oil/water separation. Cellulose, 2018, 25: 3533–3544
35 Wei H, Wang F, Qian X, et al. Superhydrophobic fluorine-rich conjugated microporous polymers monolithic nanofoam with excellent heat insulation property. Chem Eng J, 2018, 351: 856–866
36 Wang J, Geng G. Highly recyclable superhydrophobic sponge suitable for the selective sorption of high viscosity oil from water. Mar Pollut Bull, 2015, 97: 118–124